ELSEVIER

Biophysical Chemistry 125 (2007) 260–268

Biophysical Chemistry

http://www.elsevier.com/locate/biophyschem

Towards the mechanism of trimeric purine nucleoside phosphorylases: Stopped-flow studies of binding of multisubstrate analogue inhibitor — 2-amino-9-[2-(phosphonomethoxy)ethyl]-6-sulfanylpurine

B. Wielgus-Kutrowska [a], J.M. Antosiewicz [a], M. Długosz [a], A. Holý [b], A. Bzowska [a,*]

[a] *Department of Biophysics, Warsaw University, 93 Zwirki i Wigury St., Warsaw 02-089, Poland*

[b] *Institute of Organic Chemistry and Biochemistry and Centre for Novel Antivirals and Antineoplastics, 166 10 Praha 6, Flemingovo nam. 2, Czech Republic*

Received 11 July 2006; received in revised form 18 August 2006; accepted 21 August 2006
Available online 1 September 2006

Abstract

The binding of multisubstrate analogue inhibitor — 2-amino-9-[2-(phosphonomethoxy)ethyl]-6-sulfanylpurine (PME-6-thio-Gua) to purine nucleoside phosphorylase from *Cellulomonas* sp. at 20 °C, in 20 mM Hepes buffer with ionic strength adjusted to 50 mM using KCl, at several pH values between 6.5 and 8.2, was investigated using a stopped-flow spectrofluorimeter. The kinetic transients registered after mixing a protein solution with ligand solutions of different concentrations were simultaneously fitted by several association reaction models using nonlinear least-squares procedure based on numerical integration of the chemical kinetic equations appropriate for given model.

It is concluded that binding of a PME-6-thio-Gua molecule by each of the binding sites is sufficiently well described by one-step process, with a model assuming interacting binding sites being more probable than a model assuming independent sites. The association rate constants derived from experimental data, assuming one step binding and independent sites, are decreasing with an increase in pH, changing from 30 to 6 $\mu M^{-1}s^{-1}$ per binding site. The dissociation rate constants are in the range of 1–3 s^{-1}, and they are rather insensitive of changes in pH. Interestingly, for each pH value, the one-step binding model with interacting sites results in the association rate constant per site 1.5–4 times smaller for the binding of the first ligand molecule than that for the binding of the second one.

Decrease of association constants with pH indicate that the enzyme does not prefer binding of the naturally occurring anionic form of the 6-thioguanine ring (pK_a 8.7) resulting from a dissociation of N(1)–H. This finding supports the mechanism in which hydrogen bond interaction of N(1)–H with Glu204 (Glu 201 in mammalian PNPs) is crucial in the catalytic process. Results obtained also indicate that, in contrast to transition-state analogues, for which binding is followed by a conformational change, binding of multisubstrate analogue inhibitors to trimeric PNPs is a one-step process.

Keywords: PNP; PME-6-thio-Gua; Fluorescence; Stopped-flow; Numerical integration

1. Introduction

Purine nucleoside phosphorylase (PNP, E.C. 2.4.2.1) is a ubiquitous enzyme of the purine salvage metabolic pathway. In eukaryote and in some bacteria homotrimeric enzyme is present (built of three subunits with the same amino acid sequence). It catalyses the reversible phosphorolysis of 6-oxo-purine ribo- and 2′-deoxyribonucleosides, as follows:

$$\beta-(\text{deoxy})-\text{nucleoside}+\text{phosphate} \leftrightarrow \text{purine} + \alpha-(\text{deoxy})-\text{pentose}-1-\text{phosphate}.$$

Potent inhibitors of human and parasitic PNPs are considered potential immunosuppressive and anti-parasitic agents [1].

Even though the biological importance of PNP is recognised, the molecular mechanism of the enzyme is not yet fully characterised. There is still a controversy regarding the electronic/tautomeric form of the purine ring in a complex with PNP

* Corresponding author.
E-mail address: abzowska@biogeo.uw.edu.pl (A. Bzowska).

0301-4622/$ - see front matter © 2006 Elsevier B.V. All rights reserved.
doi:10.1016/j.bpc.2006.08.008

and interactions of enzyme subunits, in the ground- and in the transition-states. Interactions between enzyme subunits and conformational changes of the enzyme were documented for the transition-state events [2,3], while they do occur also in the ground-state remains to be clarified. Moreover, three proposed alternative models of catalysis differ in charge and charge distribution on the purine ring and in a role of protein–substrate hydrogen bond interactions [4–6].

In this study we analyse certain aspects of the mechanism for trimeric PNPs, namely binding of a multisubstrate analogue inhibitor — 2-amino-9-[2-(phos-phonomethoxy)ethyl]-6-sulfanylpurine (PME-6-thio-Gua, see Fig. 1) by *Cellulomonas* sp. PNP in the absence of phosphate, using stopped-flow spectrofluorimetry methods. Time resolved approach seems to be very important since steady-state titrations indicate that there are no interactions between enzyme subunits in the ground-state [7] and crystal structure of trimeric PNP from calf spleen in a complex with similar multisubstrate inhibitor revealed no structural differences between monomers composing the trimeric enzyme molecule [8].

Multisubstrate analogue inhibitors, including, PME-6-thio-Gua, are composed of three structural parts linked together: (1) purine base, (2) acyclic chain or cyclic moiety, and (3) phosphonate or phosphate or other electronegative group (see [1]). These three parts mimic substrates of PNP (see reaction scheme, above), but presence of the phosphonate group prevents approaching the transition-state. In the absence of phosphate trimeric PNPs catalyse slow hydrolysis of 6-keto-purine nucleosides and after glycosidic bond cleavage of some nucleosides substrates (e.g. inosine and guanosine but not their 7-methylated counterparts), the enzyme is trapped in the transition-state conformation in a complex with the product — purine base (e.g. hypoxantine or guanine) [2,9,10]. It is generally accepted that in the phosphorolytic reaction features of the transition-state are formed as the results of interactions of the enzyme with the purine nucleoside substrate, while presence of phosphate helps to relax the transition-state conformation and release the tightly bound purine base [9–11].

Each trimeric PNP molecule (P) contains three sites for binding of the ligand (L), one per subunit, located close to the subunit/subunit interface [5]. Because of the symmetry of the PNP trimer, the protein can be considered as a macromolecule with three identical either non-interacting or interacting sites. In our previous study we have shown that binding of guanine is a two-step process, ligand binding is followed by the conformational change of the enzyme, and also interactions between subunits occur [12].

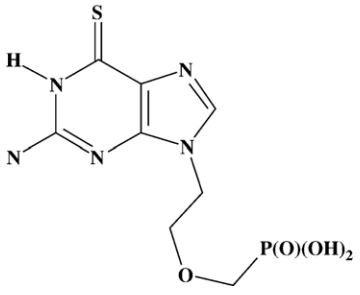

Fig. 1. Chemical structure of 2-amino-9-[2-(phosphonomethoxy)ethyl]-6-sulfanylpurine (PME-6-thio-Gua). The ligand has two groups titrating in the pH range investigated in this study: phosphonate group with $pK_a = 6.7$ for the equilibrium between monoanion and dianion, and N(1)–H of the purine ring with $pK_a = 8.7$ for the equilibrium between neutral N(1)–H form and monoanion.

The purpose of this study is to derive kinetic and optical parameters for a binding model appropriate for interaction of the symmetrical trimeric structure macromolecule with the multisubstrate analogue inhibitor i.e. the ground-state analogue, and based on these parameters, to conclude if the binding sites can be classified as interacting or non-interacting, and whether the binding by each binding site should be considered as a one-step or a two-step binding process. Recently, it was shown by analytical ultracentrifugation methods that trimeric and hexameric PNP molecules do not undergo dissociation into monomers at wide range of solution conditions, normally used in the binding studies [13,14].

Stopped-flow experiments were conducted over pH range 6.5–8.2 to see if association and dissociation rate constants are pH-dependent. These data are expected to determine the electronic/tautomeric form of the purine ring in a complex with PNP, and consequently to help in distinguishing between mechanisms proposed for trimeric PNPs.

2. Materials and methods

2.1. Materials

Commercially available PNP from *Cellulomonas* sp. (Toyobo Co., Japan), was purified on a BioCad station (PerSeptive Biosystems) by ion-exchange chromatography as described in Ref. [5], to a maximal final specific activity of 107 units/mg measured spectrophotometrically at 25 °C by the method of Kalckar with inosine as variable substrate in 50 mM phosphate buffer pH 7.0 and coupling with xanthine oxidase [15,16]. The concentration of the protein solution was determined spectrophotometrically using $\epsilon_{1\%,280\ nm} = 5.9$ [17].

Synthesis of 2-amino-9-[2-(phosphonomethoxy)ethyl]-6-sulfanylpurine (PME-6-thio-Gua) has been described elsewhere [18].

The concentrations of PME-6-thio-Gua was determined spectrophotometrically from its molar extinction coefficients at pH 7.0: $\epsilon_{\lambda=342} = 23\,800\ M^{-1}\ cm^{-1}$, assuming that it is the same as for the 6-thioguanosine [19]. Hepes, Inosine, Na_2HPO_4, $NaH_2\ PO_4$ and xanthine oxidase from buttermilk (1 unit/mg at 25 °C) were products of Sigma. All solutions were prepared with high-quality MiliQ water.

The ligand has two functional groups titrating within or close to the pH range investigated in this work. The first group is N(1)–H at the 6-thioguanine ring, with pK_a around 8.35, based on data reported in Ref. [19] for 6-thioguanosine. Our own spectrophotometric titration of PME-6-thio-Gua gives pK_a of 8.7 ± 0.1. The second group is the phosphonyl group with the secondary ionisation around $pK_a = 6.9$, reported in reference [20] for a similar compound 9-[2-(2-phosphonoethoxy)ethyl] adenine.

2.2. Instrumentation

Spectrophotometric measurements were carried out on a Uvikon 930 (Kontron, Austria) spectrophotometer, using 10-, 5-, 2- or 1-mm path-length quartz cuvettes (Hellma, Germany). Steady-state fluorescence data were recorded on a Perkin-Elmer LS-50 spectrofluorimeter (Norwalk, USA) using 4×10 mm quartz Suprasil cuvettes (Hellma). The excitation was at 290 nm and fluorescence was measured with a cut-off filter (320 nm). Both spectrometers were equipped with thermostatically controlled cell compartments. A Beckman model Φ300 pH-meter equipped with a combined semi-microelectrode and temperature sensor was used for pH determination. Stopped-flow kinetic measurements were run on a SX.18MV stopped-flow reaction analyser from Applied Photophysics Ltd. The dead time of the instrument was 1.2 ms.

2.3. Stopped-flow measurements

Emission of PNP and PNP–PME-6-thio-Gua complexes was excited at 290 nm (slit widths=0.5 mm=2.32 nm), and their fluorescence was monitored using a cut-off filter (320 nm). Extinction and emission path lengths in the stopped-flow cell were 2 mm and 10 mm, respectively.

The investigated reactions consisted of mixing equal volumes of solutions of PNP and solutions of the ligand. The concentration of the protein solution was ~0.4 μM/monomer PNP (0.133 μM/trimer). Concentrations of the ligand used in these experiments varied approximately between 0.4 and 51.2 μM. From a stock solution of the ligand, with concentration about 50 μM, seven dilutions by a factor of 2 were made, giving altogether 8 concentrations of the ligand. The measurements were done at 20 °C, at pH values of 6.5, 6.7, 7.0, 7.3, 7.6 and 8.2 in 20 mM Hepes buffer. This pH range is maximal possible for Hepes buffer. Ionic strength of all solutions was adjusted to I=50 mM using KCl. One thousand data points were recorded over the course of each reaction using oversampling option of the instrument, and usually 4–8 runs were averaged for each concentration of the reagents. Each of the 8 traces with different ligand concentrations for every pH was determined twice using separate solutions preparations.

The concentrations listed above refer to situation prior to mixing in the stopped-flow apparatus, i.e. they refer to the apparatus syringes. All solutions were filtered prior to concentration determination and subsequently degassed before placing them into the stopped-flow syringes.

2.4. Analysis of stopped-flow data

Kinetic traces, resulting from the fluorescence decrease accompanying binding of PME-6-thio-Gua to PNP, were analysed using home written software, described previously [12,21]. Two models of the reaction scheme, each treating PNP molecule as a trimer with three identical binding sites, were assumed. The first model considers binding by each of the three binding sites of PNP as a one-step process, and the second model assumes a two-step binding by each site. For each model independent and interacting binding sites were considered. Each model was related to experimental data assuming that at any given moment of time the fluorescence of the solution can be represented as a sum of contributions due to distinguishable molecular species in the mixture i.e. free protein and ligand molecules, and possible forms of their complexes:

$$F(t) = \sum_x F_x \cdot c_x(t) \tag{1}$$

where c_x is the molar concentration of molecular species X and F_x is its "molar fluorescence" for given solution conditions and the spectrofluorimeter settings. Eq. (1), together with the integration of the kinetic differential equations appropriate for the mechanism of association, described below, allows one to determine the values of the optical and kinetic parameters characterising the molecular species and their mutual conversions.

Taking into account the trimeric structure of PNP, the one-step and two-step binding by each monomer can be described by the following two sets of equations:

$$\begin{aligned} P + L &\underset{k_{d1}}{\overset{k_{a3}}{\rightleftharpoons}} C1 \\ C1 + L &\underset{k_{d2}}{\overset{k_{a2}}{\rightleftharpoons}} C2 \\ C2 + L &\underset{k_{d3}}{\overset{k_{a1}}{\rightleftharpoons}} C3 \end{aligned} \tag{2}$$

and

$$\begin{array}{ccccc} P + 3L \underset{k_{d1}}{\overset{k_{a3}}{\rightleftharpoons}} C1 + 2L \underset{k_{d2}}{\overset{k_{a2}}{\rightleftharpoons}} & C2 + L & \underset{k_{d3}}{\overset{k_{a1}}{\rightleftharpoons}} & C3 \\ \quad k_{b1} \uparrow\downarrow k_{f1} & \quad k_{b1} \uparrow\downarrow k_{f2} & & k_{b1} \uparrow\downarrow k_{f3} \\ K1 + 2L \underset{k_{d1}}{\overset{k_{a2}}{\rightleftharpoons}} C1K1 + L & \underset{k_{d2}}{\overset{k_{a1}}{\rightleftharpoons}} & C2K1 & \\ \quad k_{b2} \uparrow\downarrow k_{f1} & & k_{b2} \uparrow\downarrow k_{f2} & \\ K2 + L & \underset{k_{d1}}{\overset{k_{a1}}{\rightleftharpoons}} & C1K2 & \\ & & k_{b3} \uparrow\downarrow k_{f1} & \\ & & K3 & \end{array} \tag{3}$$

In the above two equations P is the free trimeric protein, L is the free ligand, CI is the complex of the protein with I ligand molecules with all binding sites not undergoing conformational isomerisation, KI is the complex of the protein with I ligand molecules with all binding sites after conformational isomerisation, $CIKJ$ is the complex of the protein with I+J ligand molecules, where I sites did not undergo the isomerisation and J sites are after isomerisation. Parameter k_{ai} is the association rate constant when there are i empty sites on the protein, and k_{di} is the dissociation rate constant when there are i occupied sites on the protein, k_{fi} is the transformation rate constant, with i occupied sites which have not been transformed, and k_{bi} is the reverse transformation rate constant, with i occupied and transformed sites.

The above models were fitted to the experimental data assuming the following four possibilities regarding treatment of the rate constants and the optical parameters. For the simpler reaction scheme described by Eq. (2) two possibilities were considered:

1A) The rate constants used for generation of titration curves were restricted by the relations: $k_{a3}:k_{a2}:k_{a1}=k_{d3}:k_{d2}:k_{d1}=3:2:1$, and it was assumed that each binding process is accompanied by the same increment (positive or negative) in the fluorescence. Therefore practically there are only two rate constants and one optical parameter in this model.

1B) All the rate constants and all the molar fluorescence of the different forms of the PNP–ligand complex, used in the generation of titration curves are arbitrary or adjustable.

For the more complex reaction scheme described by Eq. (3) another two possibilities were considered:

2A) The rate constants were used with the requirement that they are restricted by the relations: $k_{a3}:k_{a2}:k_{a1}=k_{d3}:k_{d2}:k_{d1}=k_{f3}:k_{f2}:k_{f1}=k_{b3}:k_{b2}:k_{b1}=3:2:1$. Therefore practically there are only 4 rate constants free to choose in the model. The "molar" optical signals of the complexes were assumed to be equal to a sum of "molar fluorescence of the free protein and the appropriate multiplication of two increments, ΔF_b for binding by one site and ΔF_t for conformational transition of one occupied site, with multiplication factors I and J, which are the number of bound ligand molecules, and the number of occupied binding sites which underwent conformational transition, respectively. Therefore practically there are only 2 optical parameters;

2B) All the rate constants and all the molar fluorescence of the different forms of the PNP–PME-6-thio-Gua complex are treated as adjustable parameters. It should be noted that even this most extensive model used in the present work restricts the number of physically justifiable parameters. For example it assumes that the isomerisation rate constant k_{b2} is the same for the complex $K2$ and $C1K2$ what might be not true in the real situation. This model contains 12 kinetic and 9 optical adjustable parameters. Without restrictions described by the above example the total number of kinetic parameters would be equal to 24.

Molar fluorescence of free PNP and free PME-6-thio-Gua at given solution conditions and stopped-flow spectrofluorimeter set-up were determined in the independent measurements and were kept constant during fitting. For PNP stock solution of 0.4 μM was mixed with buffer, and for the ligand solution with the highest concentration (app. 51.2 μM) was mixed with buffer. Besides kinetic and optical parameters described above, offset levels of the registered signals were introduced as adjustable parameters. This corrects for small fluctuations in the signal level between separate measurements and also possible small errors in preparations of subsequent ligand concentrations. The latter is expected not to lead to significant shifts as the subsequent concentrations were prepared by two-fold dilution of the preceding solution. Having offset levels as adjustable parameters also helps to keep control over the experiments as too high estimated offset correction might indicate some serious problems with our samples. In all cases reported in this work required corrections for the offset level of the kinetic traces were within fluctuations of the signals registered when collecting traces for averaging.

3. Results and discussion

In principle interactions of trimeric PNPs with their ligands are not easily followed by the fluorescence spectroscopy since such interactions do not lead to marked change of the protein intrinsic fluorescence. Typically quenching or enhancement of up to 15% of the initial fluorescence is observed upon ligand binding due to small change in the environment of the tryptophan residues [8,17,22]. These effects are not pronounced since none of the tryptophan residue present in the amino acid sequence of trimeric PNPs is located in the vicinity of the active site pocket [5,23].

One exception is the interaction with the transition-state analogue ligand–guanine, which results in puzzling marked increase of emission fluorescence with maximum at about 332–334 nm [22,17]. We have profited from this effect to develop a detailed model of interactions of trimeric PNPs with this transition-state analogue ligand [21]. The other exception are interactions with ligands that quench enzyme intrinsic fluorescence by the resonance energy transfer (FRET) mechanism. Such ligands should have absorption maximum close to the emission maximum of the enzyme fluorescence i.e. of about 340 nm. This is the case for thiopurine analogues, see e.g. Ref. [19]. We have already shown that binding of 2-amino-9-[2-

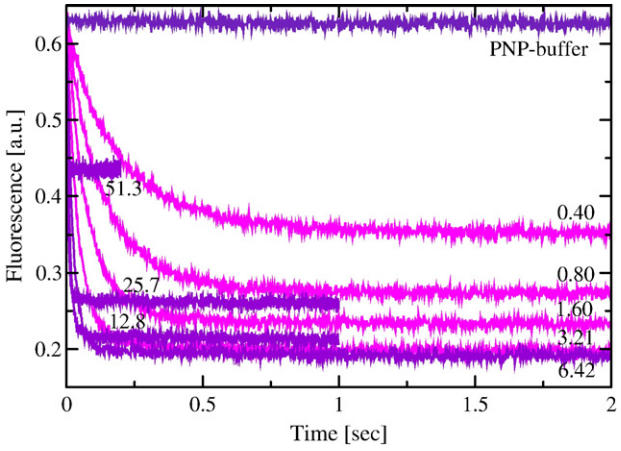

Fig. 2. Typical set of stopped-flow kinetic traces obtained after mixing of solutions of PNP and PME-6-thio-Gua. The traces shown were obtained at pH 7.3. Concentrations of the ligand (in units of [μM]) in the stopped-flow spectrometer syringe are given for each trace, corresponding concentration of PNP was 0.4 μM per monomer. In order to make the picture more clear, the traces obtained for the four lower concentrations of the ligand are drawn in different colour than the remaining four traces. The flat noisy trace on the top is for mixing PNP solution with corresponding buffer.

(phosphonomethoxy)ethyl]-6-sulfanylpurine (PME-6-thio-Gua) to purine nucleoside phosphorylase from *Cellulomonas* sp. causes marked quenching of the enzyme fluorescence and profiting from this observation we have determined the equilibrium dissociation constant for the binary complex PNP/PME-6-thio-Gua [11]. Here we study details of interactions of this analogue with trimeric PNP molecule using the stopped-flow method with the fluorescence detection of the association process.

Fig. 2 presents an example of a set of kinetic traces obtained in the stopped-flow spectrofluorimeter at pH of 7.3. Each set consists of eight mixing experiments using PNP solution with concentration of 0.4 μM per monomer and eight solutions of the ligand with concentrations increasing by factor of 2 from about 0.4 μM to about 51.2 μM. Formation of the complexes between binding sites of PNP and the ligand molecules is accompanied, as outlined above, by quenching of the fluorescence of the protein by the resonance energy transfer mechanism. However, PME-6-thio-Gua molecules contribute also in some extent, albeit rather weakly, to the observed emission signal. The fluorescence of all species: free PME-6-thio-Gua, free PNP and a complex PME-6-thio-Gua/PNP in the whole pH range investigated is presented in Fig. 3. The concentration of PNP in the cuvette was 0.2 μM per monomer and that of the ligand was 0.2, 4 and 25 μM, what corresponds to 0.4, 8, and 50 μM in the stopped-flow syringes, respectively. An increase in the fluorescence signal with increasing pH, visible for the solution containing PNP and the ligand, both at concentration of 0.2 μM (Fig. 3, triangle left), reflects a decrease in the equilibrium binding constant. This result is fully compatible with the results obtained from the stopped-flow experiments (see below). With excess ligand the fluorescence signals for mixed solutions are approximately pH independent.

Both factors, FRET of the enzyme intrinsic fluorescence in the complex with PME-6-thio-Gua and the weak fluorescence of the ligand result in a complex behaviour of the registered kinetic traces with increasing concentration of PME-6-thio-Gua. Initially each, subsequent trace has larger amplitude and its

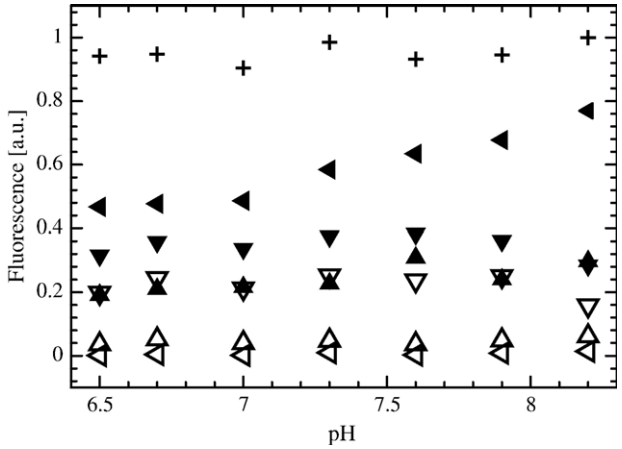

Fig. 3. Steady-state fluorescence of PNP (+), PME-6-thio-Gua (open symbols) and complex PNP/PME-6-thio-Gua (filled symbols) as a function of pH. The concentration of PNP was 0.2 μM per monomer. Concentrations of the ligand were: 0.2 μM (triangle left), 4 μM (triangle up), and 25 μM (triangle down), in the spectrofluorimeter cell.

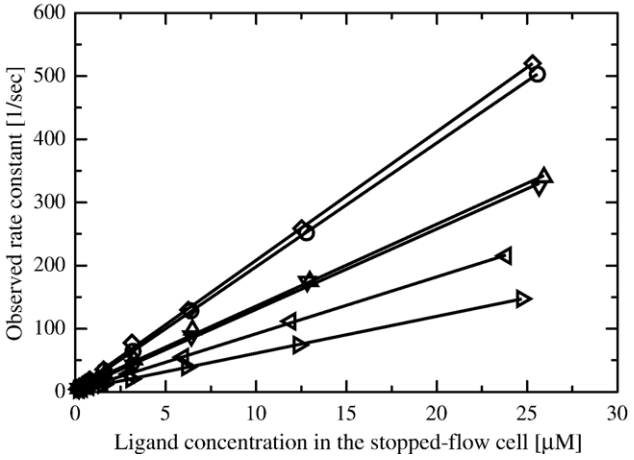

Fig. 4. Concentration dependencies of the observed rate constants obtained from single-exponent fitting to the kinetic traces registered at different pH values: 6.5 (diamond), 6.7 (circle), 7.0 (triangle up), 7.3 (triangle down), 7.6 (triangle left), and 8.2 (triangle right).

plateau region is located below the plateau region of the previous trace. Beginning from ligand concentration of about 6.5 μM in the stopped-flow syringe, the contribution of the ligand leads to a progressive up-shift of the whole trace, and also increasing part of the association reaction takes place within dead time of the stopped-flow apparatus (1.2 ms). However, even at ligand concentration of about 52 μM substantial part of the reaction is still visible (see Figs. 2 and 6).

As an initial step of data analysis, all kinetic traces were fitted to a single-exponential function:

$$I(t) = \Delta I \cdot \exp(-k_{obs} \cdot t) + I_{\infty} \quad (4)$$

where k_{obs} is the observed rate constants, ΔI is the corresponding amplitude, and I_{∞} is the final value of fluorescence. For all ligand concentrations the registered kinetic traces fit single-exponential function very well (judged by χ^2 values). Fitting of single-exponential function serves for showing that we do not observe any deviations from linear dependence of k_{obs} vs. ligand concentration in the whole range used in this study. This is shown in Fig. 4. The second purpose of using single exponential fits was to obtain rough estimates of the association and dissociation rate constants to be used as initial parameter values for nonlinear fitting procedures based on Eqs. (2) and (3) (see below).

Table 1
Parameters of model 1A, k_{a1}, k_{d1} and ΔF_{rel} as obtained from the best fits of Eq. (2) to kinetic traces registered at different pH

Parameter	pH					
	6.5	6.7	7.0	7.3	7.6	8.2
k_{a1} [μM^{-1} s^{-1}]	26.5	19.9	17.1	15.1	9.77	5.97
k_{d1} [s^{-1}]	1.97	2.19	1.87	1.66	1.70	2.88
ΔF_{rel}	−0.232	−0.237	−0.254	−0.264	−0.268	−0.272
rmsd [a.u.]	0.0647	0.0598	0.0517	0.0511	0.0539	0.0612

$\Delta F_{rel} = \Delta F / F_{PNP}$, where F_{PNP} is the fluorescence of 1 μM solution of free PNP (concentration in terms of the trimers) and ΔF is the fluorescence decrease per 1 μM following binding of a ligand molecule by a single site of trimeric PNP molecule.

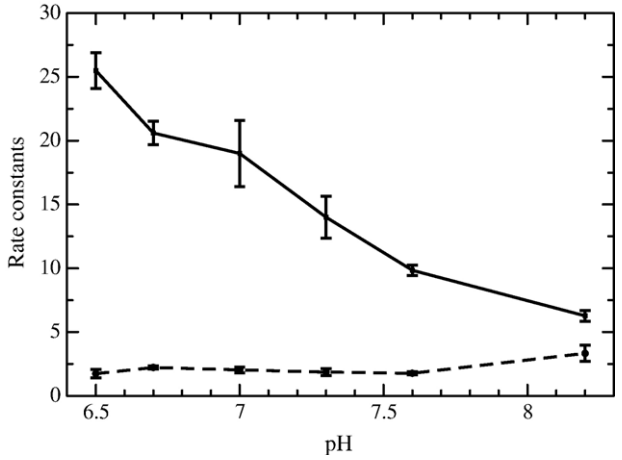

Fig. 5. pH dependence of association (experimental points connected by continuous lines, units of [μM^{-1} s^{-1}]) and dissociation (experimental points connected by dashed lines, units of [s^{-1}]) rate constants derived from model 1A. Presented values are mean of two experiments with their standard deviations.

For all pH values good linear correlation between k_{obs} and L is observed, with the lowest correlation coefficient of 0.99942 obtained for pH 7.0. This might indicate that the binding of PME-6-thio-Gua by each of the binding sites of trimeric PNP is a one-step binding process. In a case of proteins with single binding site, for one-step binding, and large excess of ligand over the protein, the dependence of k_{obs} on the total ligand concentration is linear

$$k_{obs} = k_{ass}[L] + k_{diss}, \quad (5)$$

with k_{ass} and k_{diss} being apparent association and dissociation constants, respectively, for one-step binding [24]. For a two-step binding mode by single binding site proteins, described by the equation

$$P + L \underset{k_{-1}}{\overset{k_{+1}}{\rightleftharpoons}} C \underset{k_{-2}}{\overset{k_{+2}}{\rightleftharpoons}} K \quad (6)$$

it was shown that dependence of k_{obs} versus total ligand concentration has hyperbolic saturation, with limiting $k_{obs}=k_{+2}+k_{-2}$ [24–26]. No equivalent analytical expressions exist for a multiple binding protein but one can simulate kinetic traces for assumed parameters of a two-step binding by PNP and fit them with a single-exponential function. Despite of the linear dependencies shown in Fig. 4, a two-step binding by each of the binding sites cannot be excluded because the highest observed rate constants shown there are below 550 s^{-1}. Stopped-flow technique allows one to study processes with rates up to about 1000 s^{-1}, so almost twice the largest observed rate constants determined with concentrations of PME-6-thio-Gua not exceeding 55 μM. It is possible that for ligand concentrations in the apparatus syringe larger than upper limit specified above one would observe deviations from linear correlation. This upper ligand concentration was chosen because of the contribution of the ligand to the observed signal and associated inner filter effects.

The next step in data analysis consisted of extensive fitting the measured kinetic traces with model 1A. As initial values of the kinetic parameters, we used those scattered around k_{ass} and k_{diss} derived from linear regression of k_{obs} vs. [L] according to Eq. (5). Simultaneous fits of model 1A described by Eq. (2) to the registered sets of eight kinetic transients, using programs described previously [12], resulted in reasonably good reproduction of the experimental observations. Estimated values of the parameters, together with root mean square deviations (rmsd) between experimental data and fitted traces are given in Table 1. The association rate constants obtained from model 1A are decreasing from 26.5 $\mu M^{-1}s^{-1}$ for pH 6.5 to 6 $\mu M^{-1}s^{-1}$ for pH 8.2. The dissociation rate constants obtained from these fits do not vary clearly with increasing pH. They oscillate between 1.6 and 2.9 s^{-1}. The optical signal is monotonically increasing function of pH, but the increase although steady is relatively small. Fig. 5 shows pH dependencies of association and dissociation rate constants per binding site derived from model 1A. Presented values are mean of two experiments with their standard deviations.

Results obtained for pH 7.0 may be compared with the steady-state titrations of PNP from *Cellulomonas* sp. with PME-6-thio-Gua [11]. In this experiment, with PNP concentration of 0.49 μM, $K_d=0.12\pm0.01$ μM was obtained. The present data, with assumption of one-step binding by independent sites, for pH 7.0, $k_{ass}=19.0\pm2.6$ μM^{-1} s^{-1} and $k_{diss}=2.03\pm0.23$ s^{-1}, lead to $K_d=0.11\pm0.02$ μM, hence is in very good agreement with the equilibrium dissociation constant (but see below).

Simultaneous fits of kinetic traces predicted using Eq. (2) and assuming model 1B was the next approach to interpret our experimental data. Because of large number of adjustable parameters their values derived from fitting are not as stable as in the case of model 1A. An example of best results of these fits are shown in Table 2. Regarding the pH dependence of the rate constants, basically they are similar to those obtained from model 1A but the values of the parameters are more scattered. An interesting feature of the data shown in Table 2 is that the association rate constant for binding of a second ligand molecule by individual site of trimeric PNP, i.e. $k_{a2}/2$ is larger than that for the binding of a first ligand, i.e. $k_{a3}/3$. And the rate constants for the binding of a third ligand molecule, i.e. k_{a1} are

Table 2
Parameters of model 1B, as obtained from the best fits of Eq. (2) to kinetic traces registered at different pH

Parameter	pH					
	6.5	6.7	7.0	7.3	7.6	8.2
k_{a1} [μM^{-1} s^{-1}]	17.1	16.1	10.7	10.0	3.72	2.10
$k_{a2}/2$ [μM^{-1} s^{-1}]	48.9	36.0	25.3	28.3	24.6	15.8
$k_{a3}/3$ [μM^{-1} s^{-1}]	13.3	11.1	10.4	8.60	5.60	3.67
k_{d1} [s^{-1}]	1.76	2.61	1.74	2.63	1.10	1.26
$k_{d2}/2$ [s^{-1}]	2.35	1.13	1.55	1.09	10.5	12.9
$k_{d3}/3$ [s^{-1}]	2.93	7.43	3.57	3.70	0.96	2.19
$F_{rel,C1}$	0.427	0.564	0.458	0.517	0.630	0.695
$F_{rel,C2}$	0.527	0.513	0.495	0.466	0.318	0.324
$F_{rel,C3}$	0.323	0.266	0.190	0.169	0.198	0.169
rmsd [a.u.]	0.0567	0.0494	0.0537	0.0560	0.0452	0.0505

Optical parameters are presented as relative quantities $F_{rel,x}=\Delta F_x/F_{PNP}$, where F_{PNP} is the fluorescence of 1 μM solution of free PNP (concentration in terms of the trimers) and F_x is the fluorescence per 1 μM of the form x of the complex.

approximately equal to $k_{a3}/3$. For the kinetic traces used in preparation of Table 2 the ratio of $k_{a2}/2$ to $k_{a3}/3$ is between 2.4 and 4.4. For some of the kinetic traces from repetition experiments (done with independent sample preparations) this increase is not so significant (e.g. only 1.1 for the second set of eight traces registered at pH of 7.0). Moreover, we obtained some other reasonable fits for traces employed in preparation of Table 2, where this ratio was smaller than 2–4. But on average we can conclude that this increase, when analysing experimental data with model 1B, is pretty well documented by our experiments. The values of dissociation rate constants k_{d1} are close to those obtained from model 1A, the two remaining dissociation rate constants k_{d2} and k_{d3} are rather scattered, most probably due to difficulties in fitting kinetic traces with quite large number of adjustable parameters present in model 1B.

Fig. 6 presents experimental traces obtained at pH 7.3 and traces fitted according to Eq. (2) either within framework of model 1A or model 1B. Although from Table 1 it is visible that average rmsd of both sets of the fits are of comparable value, inspection of Fig. 6 indicates that model 1B performs in one respect clearly better. For the lowest concentrations the fitted curves according to model 1A deviate significantly from the experimental counterparts, whereas for model 1B for all concentrations quality of the fitted lines is comparable among each other. This feature is the reason why we consider model of interacting sites is more probable than the model of independent sites. But because of the relatively large scattering of the rate constants derived from fitting model 1B to experimental data, it is not possible to evaluate the interaction between the binding sites precisely.

Some indication that the one-step binding model with non-interacting active sites may be a too simple approach to describe interactions of trimeric PNPs with the ground-state ligands was already present in the steady-state fluorescence titrations [8,11]. In these experiments we have noted an increase of the equilibrium dissociation constant with increasing PNP concentration. For example for the complex of PNP from *Cellulomonas* sp.

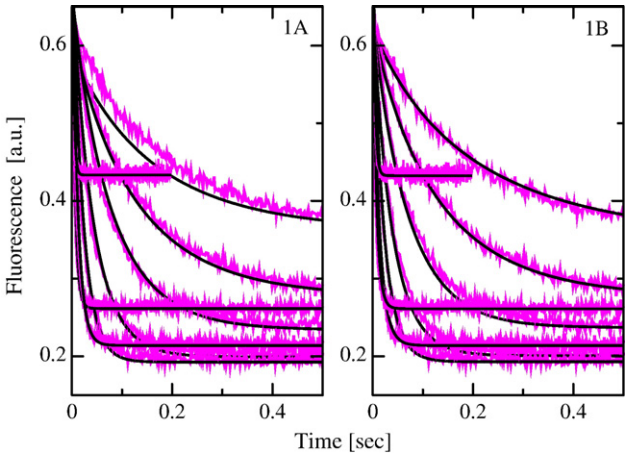

Fig. 6. Results of fitting kinetic traces obtained after mixing of solutions of PNP and PME-6-thio-Gua for high ligand concentrations, at pH 7.3, using models 1A (left) and 1B (right). Concentrations of the ligand (in units of [μM]) in the stopped-flow spectrometer syringe are given in Fig. 2. Only the first 0.5 s of the traces are shown for better clarity of the figure, because of overlap of the traces.

with PME-6-thio-Gua $K_d = 0.12 \pm 0.01$, 0.24 ± 0.02 and 0.65 ± 0.12 μM for PNP concentration 0.49, 1.41 and 4.01 μM was obtained [11].

Although, as it was discussed above, two-step binding with isomerisation rate constants below 1000 s^{-1} is not highly probable, the next model investigated by us is model 2A. It contains smaller number of adjustable parameters than model 1B. Again, for each pH value, we tried several sets of starting values of the parameters, using for the first step of binding those employed in model 1A, and for isomerisation rate constants we tried values of the order of 200–500 s^{-1}, as our observed rate constants were linear functions of the ligand concentration with maximal values being of this order of magnitude. The main feature of data obtained from these fittings is that the isomerisation rate constants are usually very high, well above possibility to be detected by stopped-flow technique and that the optical effects associated with the second step are very small. Because of very small values of the optical effects the estimated isomerisation rate constants are highly uncertain. It should be also noted that the rmsd of these fits are practically the same as the rmsd in Table 1. Similarly, application of model 2B to data analysis resulted in high isomerisation rate constants and uncertain estimates of accompanying optical effects, without substantial improvement of the rmsd. All these might indicate that association is visible by the stopped-flow technique as a one-step process.

4. Conclusions

It has been shown that kinetic traces obtained in stopped-flow spectrofluorimeter after mixing trimeric PNP from *Cellulomonas* sp. with solutions of PME-6-thio-Gua can be sufficiently well described by a one step-binding model of association with each protein's site. Hence, in contrast to interactions with the transition-state analogues, binding of ground-state analogue does not lead to protein conformational change, at least those which can be detected by transient fluorescence measurements in the millisecond time range. Inclusion of a second step in the binding using models 2A and 2B does not lead to parameters of the second step which are smooth functions of pH, neither it improves the fits substantially. The fits with two step binding have only slightly smaller rmsd values (1A vs. 2A and 1B vs. 2B), that is a result of larger number of parameters in comparison to one-step alternative. Therefore, based on the results of this study, we consider one-step binding mode of multisubstrate analogue inhibitor with either independent or interacting PNP sites as two possible alternatives justified by our experimental findings.

If interaction between the sites is taken into account, then it seems justifiable to conclude that the association rate constant for binding a second ligand molecule by trimeric PNP, for all pH values, is larger than the association rate constant for binding of the first ligand molecule. Binding of a third ligand molecule is characterised by the association rate constant close to that for the binding of a first one. This indicates some extent of positive cooperativity toward binding of PME-6-thio-Gua by PNP. However this is rather qualitative conclusion at the moment

because parameters values obtained from fitting model 1B to experimental data cannot be established with high precision. The unequivocal justification of the one-step binding model with interacting binding sites and the problem of more accurate determination of parameters of this model for trimeric PNP from *Cellulomonas* sp. or for other trimeric PNPs requires further simultaneous steady-state and time-resolved experiments for more than one ground-state analogue ligand. Since fluorescence detection is in principle not a sufficiently accurate method to be used for most of the ligands, other approaches to precisely follow the ligand binding process are desirable.

Parameters obtained in this study from one-step binding model are reasonable functions of pH. The association rate constant clearly decreases with increasing pH in the range 6.5 to 8.2, available with the hepes buffer. As outlined above PME-6-thio-Gua has two ionisable groups titrating in the pH rage investigated: phosphonate group (pK_a for monoanion/dianion the of about 6.9) and N(1)–H of the purine ring (pK_a for the neutral form/anion equilibrium of about 8.7). Hence, the pH dependence of the association constant obtained in this study (Fig. 5) indicates that the monoanionic form of the phosphonate group and the natural form of the purine ring are preferred by the enzyme, when compared with dianionic phosphonate form and the N(1)–H purine anion, respectively. This conclusion is in agreement with our previous steady-state titrations and inhibition studies of interactions with trimeric PNPs of this and similar ligands, in which pH dependence of their equilibrium dissociation constants and inhibition constants were determined [27,11] showing preference of the trimeric PNP for binding of phosphonate group in the monoanionic form and purine ring with proton at position N(1).

By contrast, PNP substrates – phosphate and ribose-1-phosphate – are bound by the trimeric phosphorylases as dianions, as shown by FTIR spectroscopy [28]. This findings underline differences noted in binding of phosphonate analogues and phosphate analogues (including fluorophoshonates better mimicking phosphate esters than the corresponding phosphonates [29]) by X-ray crystallographic studies. In the phosphate binding site the side chain of Arg84 forms a putative hydrogen bond with phosphate, see e.g. [30] and fluorinated multisubstrate analogue inhibitor [31], while in the structure with multisubstrate analogue inhibitor similar to PME-6-thio-Gua it is directed away from the active site [8].

The dissociation rate constants of PME-6-thio-Gua were found to be much less sensitive to pH changes than the association rate constants (Fig. 5) indicating that ionisable groups of the complexed ligand PME-6-thio-Gua, and functional groups in the occupied active site pocket, at least of the purine and phosphate binding sites, do not titrate in the pH range of 6.5–8.2, when the ligand and protein make the complex. This finding, in the case of the ionisable N(1)–H group of the purine base, supports the mechanism in which hydrogen bond interaction of purine ring N(1)–H with Glu204 (Glu201 in mammalian PNPs) is crucial in the catalytic process [5]. Recently this mechanism was also proposed, on the basis of new crystallographic data and solution studies, for mammalian trimeric PNPs from calf spleen [8] and from human erythrocytes [32].

Acknowledgements

We thank Lucyna Magnowska for the excellent technical assistance. This work was supported by the Ministry of Science and Higher Education (Poland, Grant No. 3P04A 03524). A.H. appreciates the financial support by the Czech Academy of Sciences (Grant No. S4055109) and of the European Union (De scsartes Prize 2002. HPAW-CT-2002-9001). The contribution to this study is a part of the IOCB project Z 40550506.

References

[1] A. Bzowska, E. Kulikowska, D. Shugar, Purine nucleoside phosphorylase: properties, functions and clinical aspects, Pharmacol. Ther. 88 (2000) 349–425.
[2] R.W. Miles, P.C. Tyler, R.H. Furneaux, C.K. Bagdassarian, V.L. Schramm, One third-the-sites transition-state inhibitors for purine nucleoside phosphorylase, Biochemisty 37 (1998) 8615–8621.
[3] F. Wang, R.W. Miles, G. Kicska, E. Nieves, V.L. Schramm, R.H. Angeletti, Immucillin-H binding to purine nucleoside phosphorylase reduces dynamic solvent exchange, Protein Sci. 9 (2000) 1660–1668.
[4] M.D. Erion, J.D. Stoeckler, W.C. Guida, R.L. Walter, S.E. Ealick, Purine nucleoside phosphorylase. 2. Catalytic mechanism, Biochemistry 36 (1997) 11735–11748.
[5] J. Tebbe, A. Bzowska, B. Wielgus-Kutrowska, Z. Kazimierczuk, W. Schröder, D. Shugar, W. Saenger, G. Koellner, Crystal structure of the purine nucleoside phosphorylase (PNP) from *Cellulomonas* sp. and its implication for the mechanism of trimeric PNPs, J. Mol. Biol. 294 (1999) 1239–1255.
[6] A. Fedorov, W. Shi, G. Kicska, E. Fedorov, P.C. Tyler, R.H. Furneaux, J.C. Hanson, G.J. Gainsford, J.Z. Larese, V.L. Schramm, S.C. Almo, Transition state structure of purine nucleoside phosphorylase and principles of atomic motion in enzymatic catalysis, Biochemistry 40 (2001) 853–860.
[7] B. Wielgus-Kutrowska, J. Frank, A. Hol, G. Koelner, A. Bzowska, Interactions of trimeric purine nucleoside phosphorylases with ground state analogues: calorimetric and fluorimetric studies, Nucleosides Nucleotides Nucleic Acids 22 (2003) 1695–1698.
[8] A. Bzowska, G. Koelner, B. Wielgus-Kutrowska, A. Stroh, G. Raszewski, A. Holý, T. Steiner, J. Frank, Crystal structure of calf spleen purine nucleoside phosphorylase with two full trimers in the asymmetric unit: important implications for the mechanism of catalysis, J. Mol. Biol. 342 (2004) 1015–1032.
[9] P.C. Kline, V.L. Schramm, Purine nucleoside phosphorylase. Inosine hydrolysis, tight binding of the hypoxanthine intermediate, and third-the-sites reactivity, Biochemistry 31 (1992) 5964–5973.
[10] A. Bzowska, Calf spleen purine nucleoside phosphorylase: complex kinetic mechanism, hydrolysis of 7-methylguanosine and oligomeric state in solution, Biochim. Biophys. Acta 1596 (2002) 293–317.
[11] B. Wielgus-Kutrowska, A. Bzowska, Probing the mechanism of purine nucleoside phosphorylase by steady-state kinetic studies and ligand binding characterisation determined by fluorimetric titrations, Biochim. Biophys. Acta 1764 (2006) 887–902.
[12] M. Dlugosz, A. Bzowska, J.M. Antosiewicz, Stopped-flow studies of guanine binding by calf spleen purine nucleoside phosphorylase, Biophys. Chem. 115 (2005) 67–76.
[13] J. Behlke, G. Koellner, A. Bzowska, Oligomeric structure of mammalian purine nucleoside phosphorylase in solution determined by analytical ultracentrifugation, Z. Naturforsch., C 60 (2005) 927–931.
[14] A. Modrak-Wojcik, K. Stepniak, V. Akoev, M. Zolkiewski, A. Bzowska, Molecular architecture of *E. coli* purine nucleoside phosphorylase studied by analytical ultracentrifugation and CD spectroscopy, Protein Sci. 15 (2006) 1794–1800.
[15] H.M. Kalckar, Differential spectrophotometry of purine compounds by means of specific enzymes: I. Determination of hydroxypurines, J. Biol. Chem. 167 (1947) 429–443.
[16] J.D. Stoeckler, R.P. Agarwal, K.C. Agarwal, R.E. Parks Jr., Purine nucleoside phosphorylase from human erythrocytes, Methods Enzymol. 51 (1978) 530–538.

[17] B. Wielgus-Kutrowska, A. Bzowska, J. Tebbe, G. Koellner, D. Shugar, Purine nucleoside phosphorylase (PNP) from *Cellulomonas* sp.: physicochemical properties, and binding of substrates determined by ligand-dependent enhancement of enzyme intrinsic fluorescence, and by protective effects of ligands on thermal inactivation of the enzyme, Biochim. Biophys. Acta 1597 (2002) 320–334.

[18] A. Holý, J. Günter, H. Dvoráková, M. Masjídková, G. Andrei, R. Snoeck, J. Balzarini, E. De Clercq, Structure-antivirial activity relationship in the series of pyrimidine and purine *N*-[2[(2-phosphonometoxy)ethyl] nucleotide analogues. Derivatives substituted at the carbon atoms of the base, J. Med. Chem. 42 (1999) 2064–2086.

[19] J.J. Fox, I. Wempen, A. Hampton, I.L. Doeerr, Thiation of Nucleosides I. Synthesis of 2-amino-6-mercapto-9-beta-D-ribofuranosylpurine ("thioguanosine") and related purine nucleosides, J. Am. Chem. Soc. 80 (1958) 1669–1674.

[20] A. Fernández-Botello, R. Griesser, A. Holý, V. Moreno, H. Sigel, Acid–base and metal–ion-binding properties of 9-[2-(2-phosphonoethoxy)-ethyl]-adenine (PEEA), a relative of the antiviral nucleotide analogue 9-[2-(phosphonomethoxy)-ethyl]-adenine (PMEA). An exercise on the quantification of isomeric complex equilibria in solution, Inorganic Chem. 44 (2005) 5104–5117.

[21] M. Długosz, E. Bojarska, J.M. Antosiewicz, A procedure for analysis of stopped-flow transients for protein-ligand association, J. Biochem. Biophys. Methods 51 (2002) 179–193.

[22] D.J.T. Porter, Purine nucleoside phosphorylase. Kinetic mechanism of the enzyme from calf spleen, J. Biol. Chem. 267 (1992) 7342–7351.

[23] G. Koelner, M. Luić, D. Shugar, W. Saenger, A. Bzowska, Crystal structure of calf spleen purine nucleoside phosphorylase in a complex with hypoxanthine at 2.15 Å resolution, J. Mol. Biol. 265 (1997) 202–216.

[24] K.A. Johnson, Transient-state kinetic analysis of enzyme reaction pathways, in: D.S. Sigman (Ed.), The Enzymes, vol. XX, Academic Press, Inc., San Diego, 1992, pp. 1–61.

[25] S. Strickland, G. Palmer, V. Massey, Determination of dissociation constants and specific rate constants of enzyme–substrate (or protein–ligand) interactions from rapid kinetic data, J. Biol. Chem. 250 (1975) 4048–4052.

[26] S.G. Rhee, P.B. Chock, Mechanistic studies of glutamine synthetase from *Escherichia coli*: kinetics of ADP and orthophosphate binding to the unadenylated enzyme, Biochemistry 15 (1976) 1755–1760.

[27] J. Wierzchowski, A. Bzowska, K. Stepniak, D. Shugar, Interactions of calf spleen purine nucleoside phosphorylase with 8-azaguanine, and a bisubstrate analogue inhibitor: implications for the reaction mechanism, Z. Naturforsch. 59c (2004) 713–725.

[28] H. Deng, A.S. Murkin, V.L. Schramm, Phosphate activation in the ground state of purine nucleoside phosphorylase, J. Am. Chem. Soc. 128 (2006) 7765S–7771S.

[29] G.M. Blackburn, D.E. Kent, Synthesis of alpha- and gamma-fluoroalkylphosphonates, J. Chem. Perkin Trans. I (1986) 913–917.

[30] C. Mao, W.J. Cook, M. Zhou, A.A. Fedorov, S.C. Almo, S.E. Ealick, Biochemistry 37 (1998) 7135–7146.

[31] M. Lui, G. Koellner, T. Yokomatsu, S. Shibuya, A. Bzowska, Calf spleen purine-nucleoside phosphorylase: crystal structure of the binary complex with a potent multisubstrate analogue inhibitor, Acta Crystallogr., D Biol. Crystallogr. 60 (2004) 1417–1424.

[32] F. Canduri, V. Fadel, L.A. Basso, M.S. Palma, D.S. Santos, W.F. de Azevedo Jr., New catalytic mechanism for human purine nucleoside phosphorylase, Biochem. Biophys. Res. Commun. 327 (2005) 646–649.